**LA-6145-MS**
Informal Report

UC-32
Reporting Date: October 1975
Issued: November 1975

# Coarse-Mesh Rebalance Methods Compatible with the Spherical Harmonic Fictitious Source in Neutron Transport Calculations

by

W. F. Miller, Jr.

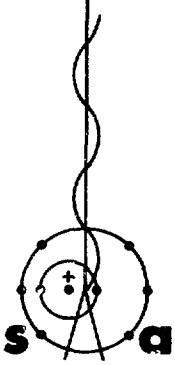

los alamos
scientific laboratory
of the University of California
LOS ALAMOS, NEW MEXICO 87545



UNITED STATES
ENERGY RESEARCH AND DEVELOPMENT ADMINISTRATION
CONTRACT W-7405-ENG. 36

In the interest of prompt distribution, this report was not edited by the Technical Information staff.

Printed in the United States of America. Available from
National Technical Information Service
US Department of Commerce
5285 Port Royal Road
Springfield, VA 22151
Price: Printed Copy $4.00 Microfiche $2.25

# COARSE-MESH REBALANCE METHODS COMPATIBLE WITH THE SPHERICAL HARMONIC FICTITIOUS SOURCE IN NEUTRON TRANSPORT CALCULATIONS

by

W. F. Miller, Jr.

ABSTRACT

The coarse-mesh rebalance method, based on neutron conservation, is used in discrete ordinates neutron transport codes to accelerate convergence of the within-group scattering source. Though very powerful for this application, the method is ineffective in accelerating the iteration on the discrete-ordinates-to-spherical-harmonics fictitious sources used for ray-effect elimination. This is largely because this source makes a minimum contribution to the neutron balance equation. In this report, the traditional rebalance approach is derived in a variational framework and compared with new rebalance approaches tailored to be compatible with the fictitious source. The new approaches are compared numerically to determine their relative advantages. We conclude that there is little incentive to use the new methods.

---

## I. INTRODUCTION

It has been observed by several authors that periodically requiring the flux to satisfy neutron balance on a phase-space grid accelerates the iteration on the within-group scattering source in discrete ordinates neutron transport calculations.[1-3] The method, used in TWOTRAN,[1] entails the superposition of a coarse spatial grid on the fine mesh and finding direction-independent factors that, when applied to the flux and current, require neutrons to be conserved in a weighted integral sense within each coarse-mesh cell. It was recognized by Lathrop[1] that his coarse-mesh rebalance equations could be derived variationally or by a weighted residual approach. Nakamura,[2] as well as Yuan et al.,[3] used variational principles and the second-order self-adjoint neutron transport equation in the derivation of their rebalance equations.

The advent of ray effect mitigating fictitious sources[4-7] has provided a new challenge to the effectiveness of coarse-mesh rebalance algorithms. The term "ray effect"[8] refers to anomalous ripples that appear in the neutron flux for some problems with isolated sources and low scattering ratios. The fictitious sources that yield spherical harmonic or spherical harmonic-like solutions effectively eliminate these distortions. However, when the within-group iteration proceeds on the sum of this source and the scattering source, the convergence properties of the iterative process are greatly degraded. As reported by Jung,[6] the traditional coarse-mesh rebalance approach is ineffective in accelerating this iteration.

In Sec. II, the step and diamond spatial differencing coarse-mesh rebalance equations are derived from a variational principle. In Sec. III, the discrete-ordinates-to-spherical-harmonics fictitious source used in this study is presented and described. In Sec. IV, variational methods are used to derive new coarse-mesh rebalance approaches more applicable to the fictitious source iteration. Section V provides numerical results while some conclusions and recommendations are described in Sec. VI.

## II. COARSE-MESH REBALANCE WITH THE STEP AND DIAMOND DIFFERENCE EQUATIONS

We variationally derive the coarse-mesh rebalance relationships that result from the step and diamond difference schemes for two reasons. First, although Lathrop[1] recognizes that a variational derivation is possible, such a procedure has not been documented to the author's knowledge. Second, the variational approach provides a unifying framework for earlier rebalance equations as well as for the new relationships derived in Sec. IV.

For simplicity, consider the monoenergetic or within-energy-group equation in x-y geometry with isotropic scattering and sources. We wish to accelerate the convergence of the so-called within-group or inner iterative process

$$\mu_m \frac{\partial \psi_m^k(x,y)}{\partial x} + \eta_m \frac{\partial \psi_m^k(x,y)}{\partial} + \sigma(x,y)\, \psi_m^k(x,y)$$

$$= \sigma_s(x,y)\, \phi^{k-1}(x,y) + Q_m(x,y) \qquad m = 1,2,\ldots M. \qquad (1)$$

These are the x-y geometry discrete ordinates equations for iteration k; a set of equations in the angular flux $\psi_m$ for each of M discrete directions determined by the direction cosine set $\{\mu_m, \eta_m\}$. In discrete ordinates neutron transport codes such as TWOTRAN, Eq. (1) is spatially differenced, traditionally with the step or the diamond difference[9] scheme, and the iteration on the scattering source proceeds. At an arbitrary stage of the iteration, neither Eq. (1) nor its corresponding set of spatially differenced equations satisfy neutron balance. This can be seen by first defining

$$\phi = \sum_{m=1}^{M} w_m \psi_m, \quad I = \sum_{m=1}^{M} w_m \mu_m \psi_m, \quad J = \sum_{m=1}^{M} w_m \eta_m \psi_m,$$

where the $\{w_m\}$ are the input quadrature weights. We then operate on Eq. (1) with $\sum_{m=1}^{M} w_m$ to obtain

$$\frac{\partial I^k}{\partial x} + \frac{\partial J^k}{\partial y} + \sigma\phi^k - \sigma_s\phi^{k-1} = Q.$$

Clearly, neutron conservation occurs only upon scalar flux convergence when $\phi^{k-1} = \phi^k$. The coarse-mesh rebalance approach is designed to speed up this convergence by requiring neutron balance in a weighted integral sense on a pre-established spatial grid.

Consider the fine-mesh spatial grid of Fig. 1 with a superimposed coarse mesh and consider the following semi-discrete functional:

$$F[\psi^*, \psi] = \int_{x_{\frac{1}{2}}}^{x_{IT+\frac{1}{2}}} dx \int_{y_{\frac{1}{2}}}^{y_{JT+\frac{1}{2}}} dy \sum_{m=1}^{M} w_m \left[\psi_m^* \right.$$

$$\left. \times \left(\mu_m \frac{\partial \psi_m}{\partial x} + \eta_m \frac{\partial \psi_m}{\partial y} + \sigma\psi_m - \sigma_s\phi - Q_m\right) - \psi_m Q_m^*\right]. \qquad (2)$$

Here, $\psi_m^*$ and $Q_m^*$ are the adjoint angular flux and adadjoint source, respectively, and as usual, we assume that all cross sections are known constants in each mesh cell. It is well known that the functional of Eq. (2) has, as one set of its Euler equations,[10] the discrete ordinates equations:

$$\mu_m \frac{\partial \psi_m}{\partial x} + \eta_m \frac{\partial \psi_m}{\partial y} + \sigma\psi_m = \sigma_s\phi + Q_m \qquad m = 1,2,\ldots M. \qquad (3)$$

The so-called Euler equations provide necessary conditions for the functional to be "stationary" with respect to arbitrary changes in $\psi_m^*$. The process of rendering a functional stationary will be pursued in more detail below. The discrete ordinates adjoint equations are also Euler equations of Eq. (2)

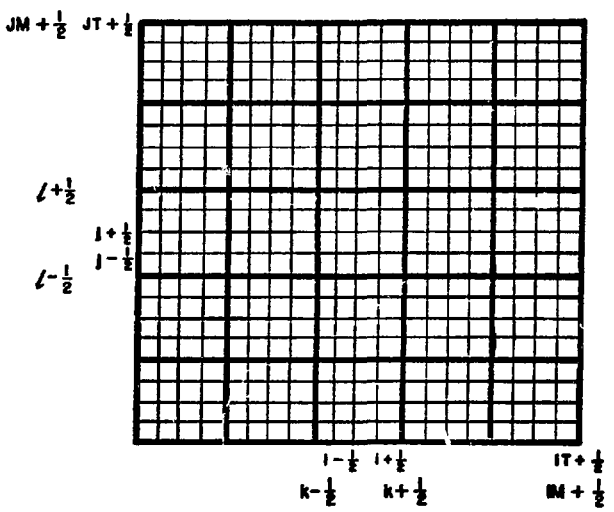


Fig. 1. Coarse and fine spatial mesh.

rendering the functionary stationary with respect to arbitrary variations in $\psi_m$.

Equation (2) may be used as a starting point to derive the coarse-mesh rebalance equations used with the step difference scheme. We begin by choosing approximation spaces for $\psi_m^*$ and $\psi_m$. Let

$$\psi_m(x,y) = \sum_{i=1}^{IT} \sum_{j=1}^{JT} f_{ij}\, \psi_{mij}\, \Delta_{mij}(x,y) \qquad (4a)$$

and

$$Q_m(x,y) = \sum_{i=1}^{IT} \sum_{j=1}^{JT} Q_{mij}\, \Delta_{mij}(x,y) \qquad (4b)$$

where

$$\Delta_{mij}(x,y) = \begin{cases} 1 & \begin{cases} x_{i-\frac{1}{2}} < x \le x_{i+\frac{1}{2}}, \\ y_{j-\frac{1}{2}} < y \le y_{j+\frac{1}{2}}, \end{cases} \quad \mu_m > 0,\ \eta_m > 0 \\ 1 & \begin{cases} x_{i-\frac{1}{2}} \le x < x_{i+\frac{1}{2}}, \\ y_{j-\frac{1}{2}} < y \le y_{j+\frac{1}{2}}, \end{cases} \quad \mu_m < 0,\ \eta_m > 0 \\ 1 & \begin{cases} x_{i-\frac{1}{2}} \le x < x_{i+\frac{1}{2}}, \\ y_{j-\frac{1}{2}} \le y < y_{j+\frac{1}{2}}, \end{cases} \quad \mu_m < 0,\ \eta_m < 0 \\ 1 & \begin{cases} x_{i-\frac{1}{2}} < x \le x_{i+\frac{1}{2}}, \\ y_{j-\frac{1}{2}} \le y < y_{j+\frac{1}{2}} \end{cases} \quad \mu_m > 0,\ \eta_m < 0 \\ 0 & \text{otherwise,} \end{cases} \qquad (4c)$$

and $\psi_{mij}$ is the angular flux for direction m and for the $ij^{th}$ mesh cell. The $\{\psi_{mij}\}$ are known from the previous iteration, while the $\{f_{ij}\}$ are unknown and are restricted by

$$f_{ij} = f_{k\ell} \qquad i\epsilon k,\ j\epsilon \ell\ . \qquad (4d)$$

We further assume

$$\psi_m^*(x,y) = \sum_{k=1}^{IM} \sum_{\ell=1}^{JM} \psi_{k\ell}^*\, \gamma_{k\ell}(x,y) \qquad (5a)$$

where

$$\gamma_{k\ell}(x,y) = \begin{cases} 1 & \begin{matrix} x_{k-\frac{1}{2}} < x < x_{k+\frac{1}{2}} \\ y_{\ell-\frac{1}{2}} < y < y_{\ell+\frac{1}{2}} \end{matrix} \\ 0 & \text{otherwise.} \end{cases} \qquad (5b)$$

Inserting Eqs. (4a) and (5a) into Eq. (2) yields the reduced functional

$$\tilde{F}[\psi^*,\psi] = \int_{x_{\frac{1}{2}}}^{x_{IT+\frac{1}{2}}} dx \int_{y_{\frac{1}{2}}}^{y_{JT+\frac{1}{2}}} dy \left[ \sum_{k=1}^{IM}\sum_{\ell=1}^{JM} \psi^*_{k\ell} \gamma_{k\ell} \left( \sum_{\mu_m>0} w_m \mu_m \sum_{i=1}^{IT}\sum_{j=1}^{JT} \left( f_{ij}\psi_{mij} - f_{i-1j}\psi_{mij} \right) \delta\left(x - x_{i-\frac{1}{2}}\right) \right.\right.$$

$$+ \sum_{\mu_m<0} w_m \mu_m \sum_{i=1}^{IT}\sum_{j=1}^{JT} \left( f_{i+1j}\psi_{mi+1j} - f_{ij}\psi_{mij} \right) \delta\left(x_{i+\frac{1}{2}} - x\right) + \sum_{\eta_m>0} w_m \eta_m \sum_{i=1}^{IT}\sum_{j=1}^{JT} \left( f_{ij}\psi_{mij} - f_{ij-1}\psi_{mij-1} \right)$$

$$\times \delta\left(y - y_{j-\frac{1}{2}}\right) + \sum_{\eta_m<0} w_m \eta_m \sum_{i=1}^{IT}\sum_{j=1}^{JT} \left( f_{ij+1}\psi_{mij+1} - f_{ij}\psi_{mij} \right) \delta\left(y_{j+\frac{1}{2}} - y\right) + \sigma \sum_{i=1}^{IT}\sum_{j=1}^{JT}\sum_{m=1}^{M} w_m f_{ij}\psi_{mij}\Delta_{\omega ij}$$

$$\left.\left. - \sigma_s \sum_{i=1}^{IT}\sum_{j=1}^{JT}\sum_{m=1}^{M} w_m f_{ij}\psi_{mij}\Delta_{mij} - \sum_{i=1}^{IT}\sum_{j=1}^{JT}\sum_{m=1}^{M} w_m Q_{mij}\Delta_{mij} \right) - \sum_{m=1}^{M} w_m Q^*_m \sum_{i=1}^{IT}\sum_{j=1}^{JT} f_{ij}\psi_{mij}\Delta_{mij} \right].$$

Carrying through the integration, we obtain

$$\tilde{F}[\psi^*,\psi] = \sum_{k=1}^{IM}\sum_{\ell=1}^{JM} \psi^*_{k\ell} \left( \sum_{j\in\ell}\sum_{\mu_m>0} w_m\mu_m \left( f_{k\ell}\psi_{mkj} - f_{k-1\ell}\psi_{mk-1j} \right) \Delta y_j + \sum_{j\in\ell}\sum_{\mu_m<0} w_m\mu_m \right.$$

$$\times \left( f_{k+1\ell}\psi_{mk+1j} - f_{k\ell}\psi_{mkj} \right) \Delta y_j + \sum_{i\in k}\sum_{\eta_m>0} w_m\eta_m \left( f_{k\ell}\psi_{mi\ell} - f_{k\ell-1}\psi_{mi\ell-1} \right) \Delta x_i + \sum_{i\in k}\sum_{\eta_m<0} w_m\eta_m$$

$$\left. \times \left( f_{k\ell+1}\psi_{mi\ell+1} - f_{k\ell}\psi_{mi\ell} \right) \Delta x_i + f_{k\ell} \sum_{i\in k}\sum_{j\in\ell} \Delta x_i \Delta y_j \sigma_{a_{ij}} \phi_{ij} - \sum_{i\in k}\sum_{j\in\ell} Q_{ij} \Delta x_i \Delta y_j \right)$$

$$+ \sum_{k=1}^{IM}\sum_{\ell=1}^{JM} f_{k\ell} \sum_{i\in k}\sum_{j\in\ell} Q^*_{ij}\phi_{ij}\Delta x_i \Delta y_j \,. \qquad (6)$$

By $\psi_{mkj}$, we refer to the angular flux evaluated at the $j^{th}$ y fine interval and at the x fine interval adjacent to the outgoing boundary of the $k^{th}$ coarse-mesh interval. A similar definition holds for $\psi_{mi\ell}$. In Eq. (6), $Q_{ij} = \sum_{m=1}^{M} w_m Q_{mij}$. To find the stationary point of the reduced functional of Eq. (6), we set

$$\frac{\partial F}{\partial \psi^*_{k\ell}} = 0$$

$k = 1, 2, \ldots IM$

$\ell = 1, 2, \ldots JM$

to obtain the coarse-mesh rebalance equations

$$f_{k\ell}(FR_{k\ell} + FL_{k\ell} + FU_{k\ell} + FD_{k\ell} + AB_{k\ell}) = QQ_{k\ell} + f_{k-1\ell} \times FR_{k-1\ell} + f_{k+1\ell}\, FL_{k+1\ell} + f_{k\ell-1}\, FU_{k\ell-1} + f_{k\ell+1}\, FD_{k\ell+1}, \qquad \begin{matrix} k=1, 2, \ldots IM \\ \ell=1, 2, \ldots JM \end{matrix} \qquad (7a)$$

where

$$FR_{k\ell} \equiv \sum_{\mu_m>0} w_m\mu_m \sum_{j\in\ell} \psi_{mkj}\Delta y_j \ ,$$

$$FL_{k\ell} \equiv \sum_{\mu_m<0} w_m|\mu_m| \sum_{j\in\ell} \psi_{mkj}\Delta y_j \ ,$$

$$FU_{k\ell} \equiv \sum_{\eta_m>0} w_m\eta_m \sum_{i\in k} \psi_{mi\ell}\Delta x_i \ ,$$

$$FD_{k\ell} \equiv \sum_{\eta_m<0} w_m|\eta_m| \sum_{i\in k} \psi_{mi\ell}\Delta x_i \ ,$$

$$AB_{k\ell} \equiv \sum_{i\in k}\sum_{j\in\ell} \sigma_{aij}\phi_{ij}\Delta x_i\Delta y_j \ ,$$

and

$$QQ_{k\ell} \equiv \sum_{i\in k}\sum_{j\in\ell} Q_{ij}\Delta x_i\Delta y_j \ . \qquad (7b)$$

Equation (7a) is the set of rebalance equations for the rebalance factors $\{f_{k\ell}\}$. Thus, after each iteration, or series of iterations, one uses the new angular flux iterate to compute the quantities of Eq. (7b), solves for the rebalance factors of Eq. (7a), and applies them as indicated in Eq. (4a) to obtain an improved flux. A weighted residual or weight-and-integrate approach may also be used to derive Eq. (7a) by first inserting Eqs. (4a) and (4b) into Eq. (3) and multiplying the result by $\gamma_{k\ell}(x,y)$. Then, operating with

$$\int_{x_{I_2}}^{x_{IT+I_2}} dx \int_{y_{I_2}}^{y_{JT+I_2}} dy \sum_{m=1}^{M} w_m \ ,$$

the desired equations result.

The coarse-mesh rebalance equations for the diamond difference scheme are derived in a manner analogous to the above procedure except Eq. (4a) is replaced by the trial solution

$$\psi_m(x,y) = \sum_{i=1}^{IT}\sum_{j=1}^{JT} f_{ij}\tilde{\psi}_{mij}(x,y)$$

where

$$\tilde{\psi}_{mij}(x,y) = \begin{cases} \psi_{mij} + \dfrac{\psi_{m_{i+I_2,j}}}{\Delta x_i}\left(x-x_{i-I_2}\right) + \dfrac{\psi_{m_{i-I_2,j}}}{\Delta x_i}\left(x_{i+I_2}-x\right) \\ + \dfrac{\psi_{m_{ij+I_2}}}{\Delta y_j}\left(y-y_{j-I_2}\right) + \dfrac{\psi_{m_{ij-I_2}}}{\Delta y_j} \\ \times \left(y_{j+I_2}-y\right), \quad x_{i-I_2}\le x\le x_{i+I_2},\ y_{j-I_2}\le y\le y_{j+I_2}, \\ 0 \text{ otherwise.} \end{cases}$$

The resulting rebalance equations are:

$$f_{k\ell}\left(FR_{k+I_2,\ell} + FL_{k-I_2,\ell} + FU_{k\ell+I_2} + FD_{k\ell-I_2} + AB_{k\ell}\right)$$
$$= f_{k-1,\ell}FR_{k-I_2,\ell} + f_{k+1,\ell}FL_{k+I_2,\ell} + f_{k,\ell-1}FU_{k\ell-I_2}$$
$$+ f_{k,\ell+1}FD_{k\ell+I_2} + QQ_{k\ell} \ . \qquad (8)$$

The flows are defined in a manner analogous to Eq. (7b). It is clear that other trial functions for $\psi_m^*$ and $\psi_m$ yield other rebalance equations.

## III. DISCRETE-ORDINATES-TO-SPHERICAL-HARMONICS FICTITIOUS SOURCE

A new development in the theory of discrete ordinates approximations is the advent of fictitious source fixups to mitigate the ray effect distortions that plague some neutron transport calculations. These fixups entail appending the within-group discrete ordinates equations of order N with a ficitious source that ensures that the resulting solution satisfies spherical harmonic or spherical harmonic-like equations of order N-1. These fictitious sources are complicated functions of the angular flux itself. Appending one of these sources alters the iterative process of Eq. (1) to:

$$\mu_m \frac{\partial \psi_m^k}{\partial x} + \eta_m \frac{\partial \psi_m^k}{\partial y} + \sigma \psi_m^k = \sigma_s \phi^{k-1} + S_{mf}^{k-1} + Q_m$$

$$m = 1, 2, \ldots M \qquad (9)$$

where $S_{mf}^{k-1}$ is the fictitious source for direction m evaluated using the angular flux from the k-1 iteration. For all fictitious sources derived in the literature,[4-7] the iterative process of Eq. (9) is slow to converge when compared to that of Eq. (1). Further, Jung et al.[6] observed that when tradiational coarse-mesh rebalance is applied to Eq. (9) with their fictitious source, the convergence rate is not significantly improved. Jung's observation is generally valid for all fictitious sources derived to date. To explain this unfavorable interaction of coarse-mesh rebalance with Eq. (9), we begin with the source due to W. F. Miller and W. H Reed:[7]

$$\begin{aligned} S_{mf} = \sum_{p=0}^{N-1} \sum_{n=0}^{p} Y_p^n(\mu_m,\eta_m) \Bigg[ & \sum_{r=0}^{N-1} \left(Y_N^r,\ \mu Y_{N-1}^r\right) \sum_{m'=1}^{M} a_{m'p}^n \\ & \times Y_N^r(\mu_{m'},\eta_{m'}) \frac{\partial \phi_{N-1}^r}{\partial x} + \sum_{r=1}^{N} \left(Y_N^r,\ \eta Y_{N-1}^{r-1}\right) \\ & \times \sum_{m'=1}^{M} a_{m'p}^n Y_N^r(\mu_{m'},\eta_{m'}) \frac{\partial \phi_{N-1}^{r-1}}{\partial y} + \sum_{r=0}^{N-2} \left(Y_N^r,\ \eta Y_{N-1}^{r+1}\right) \\ & \times \sum_{m'=1}^{M} a_{m'p}^n Y_N^r(\mu_{m'},\eta_{m'}) \frac{\partial \phi_{N-1}^{r+1}}{\partial y} + \sum_{m'=1}^{M} a_{m'p}^n \\ & \times \sum_{r=1}^{N/2} Y_N^{2r-1}(\mu_{m'},\eta_{m'}) \left(\mu_m \frac{\partial \phi_N^{2r-1}}{\partial x} + \eta_m \frac{\partial \phi_N^{2r-1}}{\partial y}\right) \Bigg]. \end{aligned} \qquad (10)$$

This fictitious source requires the solution of Eq. (9) to satisfy the spherical harmonics equations of order N-1. We have used the following inner product notation in Eq.(10): $(d,b) = \frac{1}{2} \int_{4\pi} d\Omega d(\Omega) b(\Omega)$. Also, the $Y_i^j$ are spherical harmonics and the $\{a_{mi}^j\}$ are normalized weighcs defined such that the quadrature set exactly integrates all spherical harmonics through a given order. The Appendix provides a detailed discussion of these $\{a_{mi}^j\}$.

In order to simplify Eq. (10), we define

$$\begin{aligned} F_{mmp}^n = & \sum_{r=0}^{N-1} \left(Y_N^r,\mu Y_{N-1}^r\right) \sum_{m'=1}^{M} a_{m'p}^n Y_N^r(\mu_{m'},\eta_{m'}) a_{mmN-1}^r \\ & + \sum_{m'=1}^{M} a_{m'p}^n \sum_{r=1}^{N/2} Y_N^{2r-1}(\mu_{m'},\eta_{m'}) \mu_m a_{mmN}^{2r-1} \end{aligned} \qquad (11a)$$

and

$$\begin{aligned} G_{mmp}^n = & \sum_{r=1}^{N} \left(Y_N^r,\eta Y_{N-1}^{r-1}\right) \sum_{m'=1}^{M} a_{m'p}^n Y_N^r(\mu_{m'},\eta_{m'}) a_{mmN-1}^{r-1} \\ & + \sum_{r=0}^{N/2} \left(Y_N^r,\eta Y_{N-1}^{r+1}\right) \sum_{m'=1}^{M} a_{m'p}^n Y_N^r(\mu_{m'},\eta_{m'}) a_{mmN-1}^{r+1} \\ & + \sum_{m'=1}^{M} a_{m'p}^n \sum_{r=1}^{N/2} Y_N^{2r-1}(\mu_{m'},\eta_{m'}) \eta_m a_{mmN}^{2r-1} \end{aligned} \qquad (11b)$$

These quantities depend only on the angular quadrature set used and can be precalculated before the iterative process begins. Combining Eqs. (10), (A-5), and (11), we obtain

$$S_{mf}^{(x,y)} = \sum_{p=0}^{N-1} \sum_{n=0}^{p} Y_p^n(\mu_m,\eta_m) \sum_{mm=1}^{M} \left[ F_{mmp}^n \frac{\partial \psi_{mm}^{(x,y)}}{\partial x} + G_{mmp}^n \frac{\partial \psi_{mm}^{(x,y)}}{\partial y} \right]. \qquad (12)$$

An important fact to note about Eqs. (9) and (12) is that spherical harmonic solutions are independent of the quadrature set used. Different quadrature sets do alter the solution on the system boundary slightly since they correspond to different boundary conditions. Thus, as Reed[4] has pointed out,

the potential exists to select a quadrature set that minimizes the spectral radius of the iteration matrix implied in Eq. (9). That is, we wish to select quadrature points such that $\{S_{mf}\}$ is minimized in some reasonable norm. The sheer complexity of Eq. (12), as well as its dependence on the angular flux and hence the physical problem concerned, causes such a minimization process to be impractical. The simplest approach one can take is to select quadrature points such that

$$\sum_{m=1}^{M} a_{m0}^{0} S_{mf} = 0. \tag{13}$$

Then the fictitious source is zero in a weighted sum sense. Inserting Eq. (12) into Eq. (13) yields

$$\sum_{m=1}^{M} a_{m0}^{0} S_{mf} = \sum_{p=0}^{N-1} \sum_{n=0}^{p} \sum_{mm=1}^{M} \left\{ F_{mmp}^{n} \frac{\partial \psi_{mm}}{\partial x} + G_{mmp}^{n} \frac{\partial \psi_{mm}}{\partial y} \right\}$$

$$\times \sum_{m=1}^{M} a_{m0}^{0} Y_{p}^{n}(\mu_m, \eta_m) = 0 . \tag{14}$$

But, as shown in the Appendix, the $a_{m0}^{0}$ exactly integrate all spherical harmonics through order N-1 as well as selected $N^{th}$ order ones. Thus,

$$\sum_{m=1}^{M} a_{m0}^{0} Y_{p}^{n}(\mu_m, \eta_m) = \sum_{m=1}^{M} a_{m0}^{0} Y_{0}^{0}(\mu_m, \eta_m) = 1 .$$

$$p = 0, 1, 2, \ldots N-1, \quad n = 0, 1, 2, \ldots p.$$

Hence, Eq. (14) becomes

$$\sum_{m=1}^{M} a_{m0}^{0} S_{mf} = \sum_{mm=1}^{M} \left\{ F_{mm0}^{0} \frac{\partial \psi_{mm}}{\partial x} + G_{mm0}^{0} \frac{\partial \psi_{mm}}{\partial y} \right\} = 0.$$

In general, this equation is satisfied if, and only if,

$$F_{mm0}^{0} = G_{mm0}^{0} = 0 \qquad mm=1,2,\ldots,M. \tag{15}$$

From Eq. (11), it is sufficient that the following relationships hold in order for Eq. (15) to be satisfied:

$$\sum_{m'=1}^{M} a_{m'0}^{0} Y_{N}^{r}(\mu_{m'}, \eta_{m'}) = 0, \qquad r = 0, 1, \ldots, N \tag{16a}$$

$$\sum_{m'=1}^{M} a_{m'0}^{0} Y_{N}^{2r-1}(\mu_{m'}, \eta_{m'}) \mu_{m'} = 0, \quad r = 1,2,\ldots,N/2 \tag{16b}$$

and

$$\sum_{m'=1}^{M} a_{m'0}^{0} Y_{N}^{2r-1}(\mu_{m'}, \eta_{m'}) \eta_{m'} = 0, \quad r = 1,2,\ldots,N/2. \tag{16c}$$

Spherical harmonic recursion relationships[4] can be used to express the sums of Eqs. (16b) and (16c) as sums over linear combinations of spherical harmonics of order N-1 and N+1. Since N is restricted to be even, these sums are over odd spherical harmonics. As discussed in the Appendix, symmetric quadrature sets yield a $\{a_{m0}^{0}\}$ set symmetric about $\mu = \eta = 0$, and the sums of Eqs. (16b) and (16c) are identically zero. Likewise, with a symmetric quadrature set, the sums of Eq. (16a), with r odd, are zero. We are left then with the requirement of finding a symmetric quadrature set satisfying the relationship

$$\sum_{m'=1}^{M} a_{m'0}^{0} Y_{N}^{r}(\mu_{m'}, \eta_{m'}) = 0, \quad r = 0,2,4,\ldots,N . \tag{17}$$

Two sets, discussed in the Appendix, have been derived that satisfy this requirement. Unlike the standard $S_N$ set generated in TWOTRAN, these sets result in convergence of Eq. (9) for all problems run.

Since the $\{a_{m0}^{0}\}$ are quadrature weights, Eq. (13) implies that, if the fictitious source is included in the functional of Eq. (2), its contribution is zero. Thus, quadrature sets satisfying Eq. (13) ensure that the fictitious source in no way contributes to the rebalance equations and hence the coarse-mesh rebalance equations cannot accelerate fictitious source convergence. Thus, we are lead to a dilemma. A quadrature set that satisfies Eq. (13) leads to a source for which Eq. (9) convergences more rapidly than other sets. Yet the traditional coarse-mesh rebalance method does not accelerate convergence. We are required, then, to consider variations of the traditional rebalance approaches.

## IV. REBALANCE METHODS APPLICABLE TO DISCRETE-ORDINATES-TO-SPHERICAL-HARMONICS FICTITIOUS SOURCES

Let us consider the functional of Eq. (2) with the fictitious source appended:

$$\tilde{F}[\psi^*,\psi] = \int_{x_{\frac{1}{2}}}^{x_{IT+\frac{1}{2}}} dx \int_{y_{\frac{1}{2}}}^{y_{JT+\frac{1}{2}}} dy \sum_{m=1}^{M} w_m \left\{ \psi_m^* \left( \mu_m \frac{\partial \psi_m}{\partial x} + \eta_m \frac{\partial \psi_m}{\partial y} + \sigma \psi_m - \sigma_s \phi - Q_m - S_{mf} \right) - \psi_m Q_m^* \right\}. \quad (18)$$

We have shown in the previous section that quadrature sets satisfying Eq. (17) yield a fictitious source that makes no contribution to the balance equation. That is,

$$\sum_{m=1}^{M} w_m S_{mf} = \sum_{m=1}^{M} a_{m0}^{0} S_{mf} = 0. \quad (19)$$

We have thus to seek approximation spaces for $\psi_m^*$ and $\psi_m$ such that the sums of Eq. (19) do not appear in the reduced functional. That is, we seek approximation spaces such that the fictitious source contributes to the equations for the rebalance factors.

### A. Space-Angle Coarse-Mesh Rebalance

We consider a coarse angular mesh superimposed on the fine angular mesh as indicated in Fig. 2 where, for example, the coarse mesh is composed of the four quadrants of the unit disk. We consider the simplest case of two coarse-mesh intervals, one for $\eta_m > 0$ and one for $\eta_m < 0$. In lieu of Eq. (5a), we assume

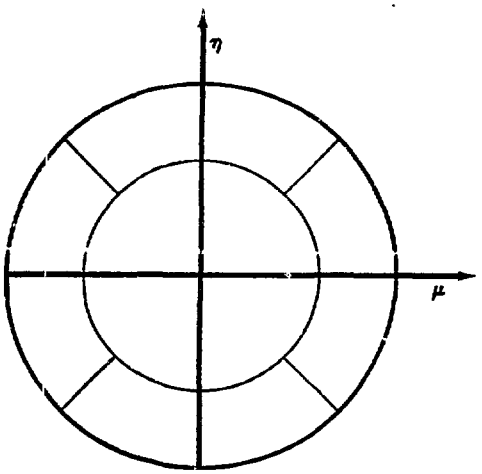


Fig. 2. Coarse and fine angular meshes.

$$\psi_m^*(x,y) = \sum_{k=1}^{IM} \sum_{\ell=1}^{JM} \bar{\psi}_{mk\ell}^* \gamma_{k\ell}(x,y) \quad (20a)$$

where $\gamma_{k\ell}(x,y)$ is defined in Eq. (5b) and

$$\bar{\psi}_{mk\ell}^* = \begin{cases} \psi_{k\ell}^{*UP} & \eta_m > 0 \\ \psi_{k\ell}^{*DN} & \eta_m < 0. \end{cases} \quad (20b)$$

Both $\psi_{k\ell}^{*UP}$ and $\psi_{k\ell}^{*DN}$ are unknown constants in m for all k,ℓ. In lieu of Eq. (4a), we use the following approximation for $\psi_m(x,y)$:

$$\psi_m(x,y) = \sum_{i=1}^{IT} \sum_{j=1}^{JT} \bar{f}_{mij} \psi_{mij} \Delta_{mij}(x,y) \quad (21a)$$

with the $\left\{\Delta_{mij}(x,y)\right\}$ given by Eq. (4c) and the $\left\{\bar{f}_{mij}\right\}$ restricted by

$$\bar{f}_{mij} = f_{k\ell}^{UP} \qquad i\epsilon k,\ j\epsilon \ell,\ \eta_m > 0 \quad (21b)$$

and

$$\bar{f}_{mij} = f_{k\ell}^{DN} \qquad i\epsilon k,\ j\epsilon \ell,\ \eta_m < 0.$$

We next combine Eqs. (18), (4b), (12), (20), and (21), differentiate $\tilde{F}\left[\psi^*,\psi\right]$ with respect to $\psi_{k\ell}^{*UP}$, and set the result to zero to obtain:

$$\begin{aligned} & f_{k\ell}^{UP}\left(FR_{k\ell}^{U} + FL_{k\ell}^{U} + FU_{k\ell} + AB_{k\ell}^{U} - FSU_{k\ell}^{RU}\right. \\ & \quad \left. + FSU_{k\ell}^{LU} - FSU_{k\ell}^{U}\right) - f_{k-1\ell}^{UP}\left(FR_{k-1\ell}^{U} - FSU_{k-1\ell}^{RU}\right) \\ & \quad - f_{k+1\ell}^{UP}\left(FL_{k+1\ell}^{U} + FSU_{k+1\ell}^{LU}\right) - f_{k\ell-1}^{UP}\left(FU_{k\ell-1} - FSU_{k\ell-1}^{U}\right) \\ & \quad - f_{k\ell}^{DN}\left(SC_{k\ell}^{D} + FSU_{k\ell}^{RD} - FSU_{k\ell}^{LD} - FSU_{k\ell}^{D}\right) \\ & \quad + f_{k-1\ell}^{DN} FSU_{k-1\ell}^{RD} - f_{k+1\ell}^{DN} FSU_{k+1\ell}^{LD} - f_{k\ell+1}^{DN} FSU_{k\ell+1}^{D} \\ & \quad = QQ_{k\ell}^{U}, \qquad k=1,2\ldots IM,\ \ell=1,2,\ldots JM \end{aligned} \quad (22a)$$

where

$$FR^{U}_{k\ell} = \sum_{j\in\ell}\sum_{\substack{\mu_m>0\\ \eta_m>0}} w_m\mu_m\psi_{mkj}\Delta y_j \ ,$$

$$FL^{U}_{k\ell} = \sum_{j\in\ell}\sum_{\substack{\mu_m<0\\ \eta_m<0}} w_m|\mu_m|\psi_{mkj}\Delta y_j \ ,$$

$$FU_{k\ell} = \sum_{i\in k}\sum_{\eta_m>0} w_m\eta_m\psi_{mi\ell}\Delta x_i$$

$$AB^{U}_{k\ell} = \sum_{i\in k}\sum_{j\in\ell}\Delta x_i\Delta y_j\left[\sigma_{ij}\sum_{\eta_m>0} w_m\psi_{mij} - \frac{\sigma_{sij}}{2}\sum_{\eta_m>0} w_m\psi_{mij}\right] \ ,$$

$$QQ^{U}_{k\ell} = \sum_{i\in k}\sum_{j\in\ell}\Delta x_i\Delta y_j\sum_{\eta_m>0} w_m Q_{mij}\Delta x_i\Delta y_j \ ,$$

$$FSU^{U}_{k\ell} = \sum_{\eta_m>0} w_m\sum_{p=0}^{N-1}\sum_{n=0}^{p} Y^n_p(\mu_m,\eta_m)\sum_{\eta_{mm}>0} G^n_{mmp}\sum_{i\in k}$$

$$\times\ \psi_{mmi\ell}\Delta x_i \ ,$$

$$FSU^{D}_{k\ell} = \sum_{\eta_m>0} w_m\sum_{p=0}^{N-1}\sum_{n=0}^{p} Y^n_p(\mu_m,\eta_m)\sum_{\eta_{mm}<0} G_{mmp}\sum_{i\in k}$$

$$\times\ \psi_{mmi\ell}\Delta x_i \ ,$$

$$FSU^{RU}_{k\ell} = \sum_{\eta_m>0} w_m\sum_{p=0}^{N-1}\sum_{n=0}^{p} Y^n_p(\mu_m,\eta_m)\sum_{\substack{\mu_{mm}>0\\ \eta_{mm}>0}} F^n_{mmp}\sum_{j\in\ell}$$

$$\times\ \psi_{mmkj}\Delta y_j \ ,$$

$$FSU^{RD}_{k\ell} = \sum_{\eta_m>0} w_m\sum_{p=0}^{N-1}\sum_{n=0}^{p} Y^n_p(\mu_m,\eta_m)\sum_{\substack{\mu_{mm}>0\\ \eta_{mm}<0}} F^n_{mmp}\sum_{j\in\ell}$$

$$\times\ \psi_{mmkj}\Delta y_j \ ,$$

$$FSU^{LU}_{k\ell} = \sum_{\eta_m>0} w_m\sum_{p=0}^{N-1}\sum_{n=0}^{p} Y^n_p(\mu_m,\eta_m)\sum_{\substack{\mu_{mm}<0\\ \eta_{mm}>0}} F^n_{mmp}\sum_{j\in\ell}$$

$$\times\ \psi_{mmkj}\Delta y_j \ ,$$

$$FSU^{LD}_{k\ell} = \sum_{\eta_m>0} w_m\sum_{p=0}^{N-1}\sum_{n=0}^{p} Y^n_p(\mu_m,\eta_m)\sum_{\substack{\mu_{mm}<0\\ \eta_{mm}<0}} F^n_{mmp}\sum_{j\in\ell}$$

$$\times\ \psi_{mmkj}\Delta y_j \ ,$$

and

$$SC^{D}_{k\ell} = \sum_{i\in k}\sum_{j\in\ell}\frac{\sigma_{sij}}{2}\Delta x_i\Delta y_j\sum_{\eta_m<0} w_m\psi_{mij} \ . \qquad (22b)$$

We repeat the above process except $F|\psi^*,\psi|$ is now differentiated with respect to $\psi^{*DN}_{k,\ell}$ to yield

$$f^{DN}_{k\ell}\left(FR^{D}_{k\ell} + FL^{D}_{k\ell} + FD_{k\ell} + AB^{D}_{k\ell} - FSD^{RD}_{k\ell} + FSD^{LD}_{k\ell} + FSD^{D}_{k\ell}\right)$$
$$- f^{DN}_{k-1\ell}\left(FR^{D}_{k-1\ell} - FSD^{RD}_{k-1\ell}\right) - f^{DN}_{k+1\ell}\left(FL^{D}_{k+1\ell} + FSD^{LD}_{k+1\ell}\right)$$
$$- f^{DN}_{k\ell+1}\left(FD_{k\ell+1} + FSD^{D}_{k\ell+1}\right) - f^{UP}_{k\ell}\left(SC^{U}_{k\ell} + FSD^{RU}_{k\ell}\right.$$
$$\left. - FSD^{LU}_{k\ell} - FSD^{U}_{k\ell}\right) + f^{UP}_{k-1\ell}\,FSD^{RU}_{k-1\ell} - f^{UP}_{k+1\ell}FSD^{LU}_{k+1\ell}$$
$$+ f^{UP}_{k\ell-1}\,FSD^{U}_{k\ell-1} = QQ^{D}_{k\ell} \ , \qquad \begin{matrix} k=1,2,\ldots,IM \\ \ell=1,2,\ldots,JM \end{matrix}$$

(23)

where the definitions of the terms appearing in Eq. (23) can be deduced from Eq. (22b). Now Eqs. (22) and (23) provide a system of 2*IM*JM linear algebraic equations for the $\left\{f^{UP}_{k\ell}\right\}$ and $\left\{f^{DN}_{k\ell}\right\}$. These rebalance factors then are applied respectively to the upward and downward directed angular fluxes. The scattering and fictitious sources are calculated from these improved fluxes and the iterative process proceeds.

Other than the obvious disadvantage of the complexity of these equations, storage requirements will be greatly increased. The quantities of Eq. (22b) must be stored over the coarse mesh. In addition, two vectors having lengths equal to the scalar flux vector are needed for application of the rebalance factors. Further, the coupled set of equations in the unknowns $\left[f^{UP}_{k\ell}\right]$ and $\left[f^{DN}_{k\ell}\right]$ will be much more difficult to solve than Eq. (7). This coarse space-angle mesh rebalance approach is discarded based upon the above observations.

B. Up-Down Coarse-Mesh Rebalance

In this approach, we retain the advantage of the space-angular mesh rebalance method, but decouple the equations for $\left[f^{UP}_{k\ell}\right]$ and $\left[f^{DN}_{k\ell}\right]$ (Eqs. (22) and (23)). In neutron transport codes such as TWOTRAN, the space-angle mesh is swept for all downward directions, assuming a known scattering and fictitious source, and then for all upward directions with the same sources. In Eq. (23), we assume that we are rebalancing on the downward directed fluxes and all upward angular fluxes are known and can be treated as sources. Then, Eq. (23) reduces to

$$f^{DN}_{k\ell}\left(FR^{D}_{k\ell} + FL^{D}_{k\ell} + FD_{k\ell} + AB^{D}_{k\ell} - FSD^{RD}_{k\ell} + FSD^{LD}_{k\ell} + FSD^{D}_{k\ell}\right) - f^{DN}_{k-1\ell}\left(FR^{D}_{k-1\ell} - FSD^{RD}_{k-1\ell}\right) - f^{DN}_{k+1\ell} \times \left(FL^{D}_{k+1\ell} + FSD^{LD}_{k+1\ell}\right) - f^{DN}_{k\ell+1}\left(FD_{k\ell+1} + FSD^{D}_{k\ell+1}\right) = \widetilde{QQ}^{D}_{k\ell}, \qquad \begin{matrix} k=1,2,\ldots IM \\ \ell=1,2,\ldots JM \end{matrix} \tag{24}$$

with

$$\widetilde{QQ}^{D}_{k\ell} \equiv QQ^{D}_{k\ell} + SC^{U}_{k\ell} + FSD^{RU}_{k\ell} - FSD^{LU}_{k\ell} - FSD^{U}_{k\ell} - FSD^{RU}_{k-1\ell} + FSD^{LU}_{k-1\ell} - FSD^{U}_{k\ell-1}.$$

In a similar manner, Eq. (22) reduces to

$$f^{UP}_{k\ell}\left(FR^{U}_{k\ell} + FL^{U}_{k\ell} + FU_{k\ell} + AB^{U}_{k\ell} - FSU^{RU}_{k\ell} + FSU^{LU}_{k\ell} - FSU^{U}_{k\ell}\right) - f^{UP}_{k-1\ell}\left(FR^{U}_{k-1\ell} - FSU^{RU}_{k-1\ell}\right) - f^{UP}_{k+1\ell}\left(FL^{U}_{k+1\ell} + FSU^{LU}_{k+1\ell}\right) - f^{UP}_{k\ell-1}\left(FU_{k\ell-1} - FSU^{U}_{k\ell-1}\right) = \widetilde{QQ}^{U}_{k\ell}, \qquad \begin{matrix} k=1,2,\ldots IM \\ \ell=1,2,\ldots JM \end{matrix} \tag{25}$$

with

$$\widetilde{QQ}^{U}_{k\ell} = QQ^{U}_{k\ell} + SC^{D}_{k\ell} + FSU^{RD}_{k\ell} - FSU^{LD}_{k\ell} - FSU^{D}_{k\ell} - FSU^{RD}_{k-1\ell} + FSU^{LD}_{k+1\ell} + FSU^{D}_{k\ell+1}.$$

Equations (24) and (25) are significantly more simple to solve than the space-angular mesh rebalance equations. The storage requirements are still significantly larger than that needed in the traditional rebalance method, though if only a reasonably coarse mesh is used, the storage penalty is not great. Intuitively, one would expect less acceleration than with the space-angular mesh equations since the coupling in $\left[f^{up}_{k\ell}\right]$ and $\left[f^{DN}_{k\ell}\right]$ is less.

Equations (24) and (25) may be further simplified by ignoring the fact that the fictitious source is comprised of spatial derivatives when deriving the acceleration scheme. Then, there is no spatial coupling in $\left[f^{UP}_{k\ell}\right]$ or $\left[f^{DN}_{k\ell}\right]$ in the fictitious source term. Then, Eq. (24) becomes

$$f^{DN}_{k\ell}\left(FR^{D}_{k\ell} + FL^{D}_{k\ell} + FD_{k\ell} + AB^{D}_{k\ell} - \overline{FSD}^{D}_{k\ell}\right) - f^{DN}_{k-1\ell}\,FR^{D}_{k-1\ell} - f^{DN}_{k+1\ell}\,FL^{D}_{k+1\ell} - f^{DN}_{k\ell+1}\,FD_{k\ell+1} = \widetilde{QQ}^{D}_{k\ell}, \qquad \begin{matrix} k=1,2,\ldots,IM \\ \ell=1,2,\ldots,JM \end{matrix} \tag{26}$$

while Eq. (25) is

$$f^{UP}_{k\ell}\left(FR^{U}_{k\ell} + FL^{U}_{k\ell} + FU_{k\ell} + AB^{U}_{k\ell} - \overline{FSU}^{U}_{k\ell}\right) - f^{UP}_{k-1\ell}\,FR^{U}_{k-1\ell} - f^{UP}_{k+1\ell}\,FL^{U}_{k+1\ell} - f^{UP}_{k\ell-1}\,FU_{k\ell-1} = \widetilde{QQ}^{U}_{k\ell}. \tag{27}$$

In these expressions, the definitions of Eq. (22b) apply and

$$\overline{FSD}^{D}_{k\ell} = FSD^{RD}_{k\ell} - FSD^{LD}_{k\ell} - FSD^{D}_{k\ell} - FSD^{RD}_{k-1\ell} + FSD^{LD}_{k+1\ell} + FSD^{D}_{k\ell+1},$$

and

$$\overline{FSU}^{U}_{k\ell} = FSU^{RU}_{k\ell} - FSU^{LU}_{k\ell} - FSU^{U}_{k\ell} - FSU^{RU}_{k-1\ell} + FSU^{LU}_{k+1\ell} - FSU^{U}_{k\ell-1}.$$

We would expect a less effective acceleration scheme than that of Eqs. (24) and (25) due to the decreased spatial coupling of the rebalance factors.

C. Angular Moment Coarse-Mesh Rebalance

We stated in Sec. III, and will demonstrate in Sec. IV, that quadrature sets that satisfy Eq. (13), when used in conjunction with Eq. (9), yield an iterative scheme that generally converges more rapidly than when the standard $S_N$ scheme is used. However, standard rebalance methods, based on the neutron conservation equation, are ineffective. Since the fictitious source makes no contribution to this equation, we consider an equation involving higher angular moments. First, let $\sum_{pn}$ denote the sum over all spherical harmonic orders for which, in general,

$$\sum_{m=1}^{M} a_{mp}^{n} S_{mf}^{(x,y)} \neq 0.$$

These orders may easily be determined numerically for a given quadrature set as discussed in the Appendix. Then assume

$$\psi_m^*(x,y) = \frac{1}{w_m} \sum_{k=1}^{IM} \sum_{\ell=1}^{JM} \psi_{k\ell}^* \gamma_{k\ell}(x,y) \sum_{pn} a_{mp}^{n} , \qquad (28)$$

and let

$$\psi_m(x,y) = \sum_{i=1}^{IT} \sum_{j=1}^{JT} f_{ij} \psi_{mij} \Delta_{mij}(x,y) , \qquad (29)$$

with $\left[\Delta_{mij}\right]$ and $\left[f_{ij}\right]$, respectively, satisfying Eqs. (4c) and (4d). Inserting Eqs. (28) and (29) into Eq. (2) differentiating $F\left[\psi^*,\psi\right]$ with respect to $\psi_{k\ell}^*$ and setting the results to zero yields

$$f_{k\ell}\left(\widetilde{FR}_{k\ell} + \widetilde{FL}_{k\ell} + \widetilde{FU}_{k\ell} + \widetilde{FD}_{k\ell} + \widetilde{AB}_{k\ell}\right) - f_{k-1\ell}\,\widetilde{FR}_{k-1\ell} - f_{k+1\ell}\,\widetilde{FL}_{k+1\ell} - f_{k\ell-1}\,\widetilde{FU}_{k\ell-1} - f_{k\ell+1}\,\widetilde{FD}_{k\ell+1} = \widetilde{QQ}_{k\ell} \qquad \begin{matrix} k=1,2,\ldots,IM \\ \ell=1,2,\ldots,JM \end{matrix} \qquad (30a)$$

where

$$\widetilde{FR}_{k\ell} = \sum_{\mu_m>0} \sum_{pn} a_{mp}^{n} \mu_m \sum_{j\in\ell} \psi_{mkj} \Delta y_j - \sum_{m=1}^{M} \sum_{pn} a_{mp}^{n} \cdot$$

$$\times \sum_{p'=1}^{N-1} \sum_{n'=1}^{p'} Y_{p'}^{n'}\left(\mu_m,\eta_m\right) \sum_{\mu_{mm}>0} F_{mmp'}^{n'} \sum_{j\in\ell} \psi_{mmkj} \Delta y_j ,$$

$$\widetilde{FL}_{k\ell} = \sum_{\mu_m<0} \sum_{pn} a_{mp}^{n} |\mu_m| \sum_{j\in\ell} \psi_{mkj} \Delta y_j + \sum_{m=1}^{M} \sum_{pn} a_{mp}^{n}$$

$$\times \sum_{p'=1}^{N-1} \sum_{n'=1}^{p'} Y_{p'}^{n'}\left(\mu_m,\eta_m\right) \sum_{\mu_{mm}<0} F_{mmp'}^{n'} \sum_{j\in\ell} \psi_{mmkj} \Delta y_j ,$$

$$\widetilde{FU}_{k\ell} = \sum_{\eta_m>0} \sum_{pn} a_{mp}^{n} \eta_m \sum_{i\in k} \psi_{mi\ell} \Delta x_i - \sum_{m=1}^{M} \sum_{pn} a_{mp}^{n}$$

$$\times \sum_{p'=1}^{N-1} \sum_{n'=1}^{p'} Y_{p'}^{n'}\left(\mu_m,\eta_m\right) \sum_{\eta_{mm}>0} G_{mmp'}^{n'} \sum_{i\in k} \psi_{mmi\ell} \Delta x_i ,$$

$$\widetilde{FD}_{k\ell} = \sum_{\eta_m<0} \sum_{pn} a_{mp}^{n} |\eta_m| \sum_{i\in k} \psi_{mi\ell} \Delta x_i + \sum_{m=1}^{M} \sum_{pn} a_{mp}^{n}$$

$$\times \sum_{p'=1}^{N-1} \sum_{n'=1}^{p'} Y_{p'}^{n'}\left(\mu_m,\eta_m\right) \sum_{\eta_{mm}<0} G_{mmp'}^{n'} \sum_{i\in k} \psi_{mmi\ell} \Delta x_i ,$$

$$\widetilde{AB}_{k\ell} = \sum_{m=1}^{M} \sum_{pn} a_{mp}^{n} \sum_{i\in k} \sum_{j\in\ell} \left(\sigma_{ij}\psi_{mij} - \sigma_{sij}\phi_{ij}\right) \Delta x_i \Delta y_j ,$$

and

$$\widetilde{QQ}_{k\ell} = \sum_{m=1}^{M} \sum_{pn} a_{mp}^{n} \sum_{i\in k} \sum_{j\in\ell} Q_{mij} \Delta x_i \Delta y_j . \qquad (30b)$$

In principal, this scheme requires no more computer storage than standard rebalance, though if one desires the true absorptions and flows to be printed, one more sweep through the space-angle mesh is needed after convergence.

A simplification analogous to that applied in the previous section to up-down rebalance may be applied to the angular moment rebalance equations. That is, the fictitious source may be treated as if it did not involve derivatives, thus eliminating coupling in $\left[f_{k\ell}\right]$ for these terms. Equation (30a) then reduces to

$$f_{k\ell}\left(FR'_{k\ell} + FL'_{k\ell} + FU'_{k\ell} + FD'_{k\ell} + AB'_{k\ell}\right) - f_{k-1\ell} \times FR'_{k-i\ell} - f_{k+1\ell}\, FL'_{k+1\ell} - f_{k\ell-1}\, FU'_{k\ell-1} - f_{k\ell+1}\, FD'_{k\ell+1} = \widetilde{QQ}_{k\ell}\,, \qquad \begin{matrix} k=1,2,\ldots,IM \\ \ell=1,2,\ldots,JM \end{matrix} \qquad (31)$$

where the flows are the same of those of Eq. (30b) without the fictitious source contributions, and

$$AB'_{k\ell} = \widetilde{AB}_{k\ell} - \sum_{m=1}^{M} \sum_{pn} a^{n}_{mp} \sum_{p'=1}^{N-1} \sum_{n'=1}^{p'} Y^{n'}_{p'}\left(\mu_m, \eta_m\right)$$

$$\times \left( \sum_{\mu_{mm}>0} F^{n'}_{mmp'} \sum_{j\in\ell} \left(\psi_{mmkj} - \psi_{mmk-1j}\right)\Delta y_j + \sum_{\mu_{mm}<0} \right.$$

$$\times F^{n'}_{mmp'} \sum_{j\in\ell} \left(\psi_{mmk+1j} - \psi_{mmkj}\right)\Delta y_j + \sum_{\eta_{mm}>0} G^{n'}_{mmp'}$$

$$\times \sum_{i\in k} \left(\psi_{mmi\ell} - \psi_{mmi\ell-1}\right)\Delta x_i + \sum_{\eta_{mm}<0} G^{n'}_{mmp'} \sum_{i\in k}$$

$$\left. \times \left(\psi_{mmi\ell+1} - \psi_{mi\ell}\right)\Delta x_i \right).$$

Again, we expect Eq. (31) to be less effective in accelerating when compared to Eq. (30a) due to the tighter spatial coupling of $\left|f_{k\ell}\right|$ in the latter case.

## V. NUMERICAL RESULTS

In this section, we consider several sample problems in order to compare the quadrature sets and acceleration schemes described in the previous sections. We also consider both the diamond and step spatial differencing schemes. For all problems run, the pointwise convergence criterion was $10^{-3}$ and the fictitious source used was that one which converts the discrete ordinates equations of order four to the spherical harmonics equations of order three. The three problems run are depicted in Figs. 3-5 with region cross sections provided in Table I. We used a spatial mesh, with equal intervals, of 20 x 20, 30 x 30, and 20 x 20, respectively, for problems 1-3.

Table II provides a comparison of the number of inner iterations [see Eq. (9)] required for convergence using the step and diamond schemes with no

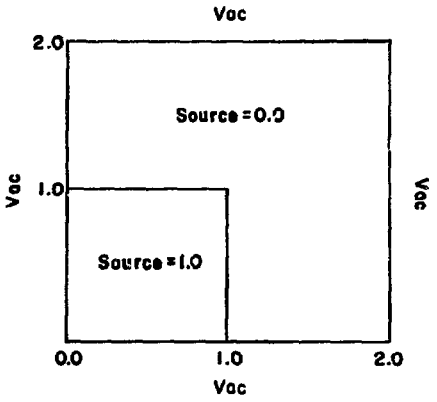


Fig. 3. Test problem 1.

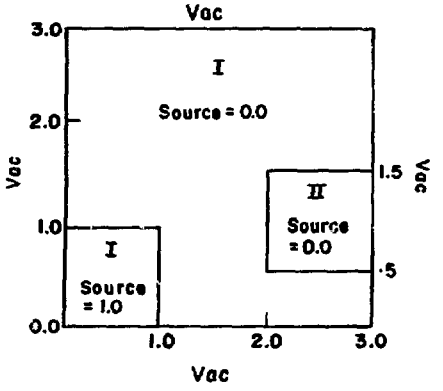


Fig. 4. Test problem 2.

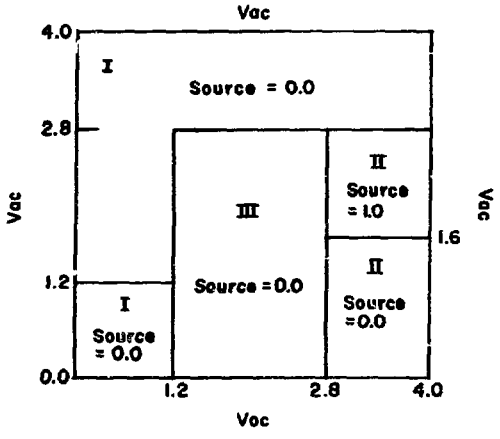


Fig. 5. Test problem 3.

TABLE I

CROSS SECTIONS FOR TEST PROBLEMS

| Cross Section | Problem 1 | Problem 2 | | Problem 3 | | |
|---|---|---|---|---|---|---|
| | | Reg. I | Reg. II | Reg. I | Reg. II | Reg. III |
| $\sigma_a$ | 1.0 | 0.5 | 0.10 | 1.0 | 0.0 | 0.0 |
| $\sigma_t$ | 1.0 | 0.75 | 1.0 | 1.0 | 1.0 | 0.01 |
| $\sigma_s$ | 0.0 | 0.25 | 0.90 | 0.0 | 1.0 | 0.01 |
| $\nu\sigma_f$ | 0.0 | 0.0 | 0.0 | 0.0 | 0.0 | 0.0 |

TABLE II

ITERATIONS REQUIRED FOR CONVERGENCE WITH VARIOUS QUADRATURE SETS AND DIFFERENCE SCHEMES

| Problem | Step Difference Scheme | | | | Diamond Scheme | |
|---|---|---|---|---|---|---|
| | Quad Set 1 | Quad Set 2 | Quad Set 3 | Quad* Set 3 | Quad Set 2 | Quad Set 3 |
| 1 | 19 | 19 | 18 | 18 | 29 | >50 |
| 2 | 22 | 21 | 21 | 21 | 45 | >50 |
| 3 | 30 | 31 | 31 | 31 | >50 | >50 |

*This problem was run with coarse-mesh rebalance.

iteration acceleration mechanism employed. Quadrature Sets 1 and 2 are those discussed in the Appendix, while Set 3 is the standard $S_N$ set used in TWOTRAN.[1] While the first two sets satisfy Eq. (13), the $S_N$ set does not. This does not appear to affect the iteration count when the step scheme is used. When the diamond scheme is used in conjunction with Set 3, however, the iteration diverges for all problems run. The first two sets, although requiring more iterations for convergence than with the step scheme, yield convergent algorithms when used with the diamond scheme. Since Set 3 does not satisfy Eq. (13), the fictitious source does contribute to the neutron balance equation. Included in Table II are the results of runs using coarse-mesh rebalance and Set 3. The number of iterations is unaffected largely due to the fact that, although the contribution of the fictitious source to the rebalance equations is not zero, it is very small. Table II then provides little basis to make a quadrature set selection when the step scheme is used but clearly indicates that schemes satisfying Eq. (13) are preferable when the diamond scheme is used.

One reason for the better performance of all sets when used with the step scheme is related to the behavior of the analytic solution of the spherical harmonics equations at material interfaces. It is well known that certain angular flux moments are discontinuous at material interfaces with the spherical harmonics method.[7] Yet the diamond difference approximation imposes angular flux continuity at the mesh cell boundaries. The step scheme, however, allows angular flux, and hence flux moment, discontinuity at all mesh cell edges.

Table III depicts an iteration count comparison for three of the methods discussed in Sec. IV. Method 1 is the up-down coarse-mesh rebalance approach described by Eqs. (24) and (25). Method 2 is the simplification of Method 1 given by Eqs. (26) and (27). Method 3 is the angular moment coarse-mesh rebalance approach of Eq. (31). All problems were run with quadrature Set 1 and the step scheme. When the iteration counts are compared with the nonacceleration results (see Column 1 of Table II), it is clear that none of the proposed methods are very effective in accelerating the iteration process.

## VI. CONCLUSIONS AND RECOMMENDATIONS

In this work we have sought coarse-mesh rebalance methods that accelerate the iteration on the fictitious source (Eq. (9)). Although we have developed several seemingly promising methods, none of the proposed procedures is effective enough to warrant consideration for production codes. Since coarse-mesh rebalance methods are nonlinear and the fictitious source is extremely complicated, it is very difficult to determine the reasons for the disappointing results. It appears from the results,

TABLE III

COMPARISON OF ITERATION COUNTS USING PROPOSED REBALANCE METHODS

| Problem | Method 1 | | Method 2 | | Method 3 | |
|---|---|---|---|---|---|---|
| | System | Fine | System | Fine | System | Fine |
| 1 | 19 | 18 | 19 | 19 | 19 | 19 |
| 2 | 21 | 20 | 22 | 21 | 22 | 21 |
| 3 | 30 | 28 | 30 | 29 | 30 | 29 |

however, that the coarse-mesh rebalance approach to accelerating Eq. (9) should be discarded in favor of a synthetic[12] or some other approach.

REFERENCES


1. K. D. Lathrop and F. W. Brinkley, "TWOTRAN-II: An Interfaced, Exportable Version of the TWOTRAN Code for Two-Dimensional Transport," Los Alamos Scientific Laboratory report LA-4848-MS (July 1973).

2. S. Nakamura, " Variational Rebalancing Method for Linear Iterative Convergence Schemes of Neutron Diffusion and Transport Equations," Nucl. Sci. Eng. 39, 278 (1970).

3. Y. C. Yuan, E. E. Lewis, and W. F. Miller, Jr., "Iterative Solution Methods for Two-Dimensional Finite Element Approximations in Neutron Transport," Proc. Conf. Computational Methods in Nuclear Engineering, CONF-750413, Charleston, SC, III-85 (1975).

4. W. H. Reed, "Spherical Harmonic Solutions of the Neutron Transport Equation from Discrete Ordinate Codes," Nucl. Sci. Eng. 49, 10 (1972).

5. K. D. Lathrop, "Elimination of Ray Effects by Converting Discrete Ordinate Equations to Spherical Harmonic-Like Equations," Proc. Conf. New Dev. in Reactor Math. and Applications, Idaho Falls, ID (March 1971).

6. J. Jung, H. Chijiwa, K. Kobayaski, and H. Nishihara, "Discrete Ordinate Neutron Transport Equation Equivalent to $P_L$ Approximation," Nucl. Sci. Eng. 49, 1 (1972).

7. W. F. Miller, Jr., and W. H. Reed, "Discrete Ordinate-to-Spherical Harmonic Conversions for Ray Effect Mitigation in X-Y Geometry," Proc. Conf. Computational Methods in Nuclear Engineering, CONF-750413, Charleston, SC, III-101 (1975).

8. K. D. Lathrop, "Ray Effects in Discrete Ordinates Equations," Nucl. Sci. Eng. 32, 357 (1968).

9. K. D. Lathrop, "Spatial Differencing of the Transport Equation: Positivity vs Accuracy," J. Comp. Phys. 4, 475 (1969).

10. R. Courant, and D. Hilbert, Methods of Mathematical Physics, Vol. 1, (Interscience Publishers, Inc., NY, 1961).

11. B. G. Carlson, "Tables of Symmetric Equal Weight Quadrature $EQ_N$ over the Unit Sphere," Los Alamos Scientific Laboratory report LA-5952 (1975).

12. W. H. Reed, "The Effectiveness of Acceleration Techniques for Iterative Methods in Transport Theory," Nucl. Sci. Eng. 45, 245-254 (1971).


---

## APPENDIX

## DETERMINATION OF SPHERICAL HARMONIC QUADRATURE WEIGHTS

In the derivation of the Miller-Reed fictitious source, the angular flux is assumed to have a spherical harmonic polynomial expansion given by

$$\psi(x,y,\mu,\eta) = \sum_{p=0}^{N-1} \sum_{n=0}^{p} Y_p^n(\mu,\eta)\phi_p^n(x,y) + \sum_{n=1}^{N/2} x\, Y_N^{2n-1}(\mu,\eta)\phi_N^{2n-1}(x,y) \qquad (A\text{-}1)$$

where the Y's are spherical harmonic polynomials defined by

$$Y_p^n = \left[\frac{\left(2-\delta_{n,0}\right)\left(p-n\right)!\left(2p+1\right)}{2\pi(p+n)!}\right]^{\frac{1}{2}} P_p^n(\mu)\cos n\phi. \qquad (A\text{-}2)$$

Here $\mu$ is the x-component of the neutron direction vector, while the y-component is

$$\eta = \sqrt{1-\mu^2}\cos\phi\ .$$

The $P_p^n(\mu)$ are associated Legendre polynomials. The spherical harmonics are normalized such that

$$\left(Y_p^n,\ Y_{p'}^{n'}\right) = \int_{-1}^{1} d\mu \int_0^{\pi} d\phi\ Y_p^n\, Y_{p'}^{n'} = \delta_{pp'}\delta_{nn'}.$$

The spherical harmonic angular flux moments, $\phi_p^n$, are defined by

$$\left(\psi,\ Y_p^n\right) = \phi_p^n\ .$$

A Lagrange basis is introduced such that the unknowns are directional fluxes in lieu of angular flux moments. Thus, in addition to Eq. (A-1), we also set

$$\psi(x,y,\mu,\eta) = \sum_{m=1}^{M} \psi_m(x,y)\, L_m(\mu,\eta) \ , \qquad \text{(A-3)}$$

where the $\{L_m\}$ are Langrange polynomials and M is the number of directions corresponding to the discrete ordinates order, N. To find these polynomials in terms of the spherical harmonics, we expand the $\{L_m\}$ by

$$L_m(\mu,\eta) = \sum_{p=0}^{N-1} \sum_{n=0}^{p} a_{mp}^{n}\, Y_p^n + \sum_{n=1}^{N/2} a_{mN}^{2n-1}\, Y_N^{2n-1} \ . \qquad \text{(A-4)}$$

Combining Eqs. (A-1), (A-3), and (A-4), it is clear that

$$\phi_p^n = \sum_{m=1}^{M} a_{mp}^{n}\, \psi_m \ . \qquad \text{(A-5)}$$

To find the $\{a_{mp}^n\}$, we define the MxM matrices.

$$Y = \begin{Bmatrix} Y_0^0(\mu_1,\eta_1)\, Y_1^0(\mu_1,\eta_1) \cdots Y_N^{N-1}(\mu_1,\eta_1) \\ Y_0^0(\mu_2,\eta_2)\, Y_1^0(\mu_2,\eta_2) \cdots Y_N^{N-1}(\mu_2,\eta_2) \\ \cdot \\ \cdot \\ \cdot \\ Y_0^0(\mu_M,\eta_M)\, Y_1^0(\mu_M,\eta_M) \cdots Y_N^{N-1}(\mu_M,\eta_M) \end{Bmatrix}$$

and

$$A = \begin{Bmatrix} a_{1_0}^0\ a_{2_0}^0 \cdots a_{M_0}^0 \\ a_{1_1}^0\ a_{2_1}^0 \cdots a_{M_1}^0 \\ \cdot \\ \cdot \\ \cdot \\ a_{1_N}^{N-1} \cdots a_{M_N}^{N-1} \end{Bmatrix} .$$

Then, it follows from Eq. (A-4) and the definition of Lagrange polynomials, that

$$YA = I \qquad \text{(A-6)}$$

where I is the identity matrix. Thus, the A array is determined completely from the quadrature points and is given by

$$A = Y^{-1} \ . \qquad \text{(A-7)}$$

It is difficult to deduce anything about the structure of $Y^{-1}$ for a given quadrature set. However, certain generalities can be made about the matrix A based on numerical experimentation with several sets, including the ones to be presented below. The first observation follows from Eqs. (A-2) and (A-4):

$$\sum_{m=1}^{M} a_{m0}^0 = \sqrt{2\pi} \sum_{m=1}^{M} a_{m0}^0\, Y_0^0(\mu_m,\eta_m) = \sqrt{2\pi} \ .$$

Second, all the $\{a_{m0}^0\}$ are positive and are analogous to quadrature weights, since, from Eq. (A-5),

$$\phi_0^0 = \sum_{m=1}^{M} a_{m0}^0 \psi_m \ .$$

Thus, note that these quadrature "weights" are fixed by the quadrature points. Third, for a quadrature set symmetric about $\mu = \eta = 0$, the $a_{m0}^0$ are likewise symmetric about $\mu = \eta = 0$.

As shown in Sec. III, there are incentives for deriving symmetric quadrature sets that satisfy Eq. (17), repeated here

$$\sum_{m=1}^{M} a_{m0}^0\, Y_N^r(\mu_m,\eta_m) = 0 \qquad r=0,2,4,\ldots,N. \qquad \text{(A-8)}$$

We take the specific case of N = 4 and point out sets that satisfy Eq. (A-8).

1. Quadrature Set 1--The first quadrature set satisfying Eq. (A-8) is the EQN set derived by Carlson.[11] This set is

| m | $w_m$ | $\mu_m$ | $\eta_m$ |
|---|---|---|---|
| 1 | 0.0833333 | 0.3500212 | 0.3500212 |
| 2 | 0.8333333 | 0.3500212 | 0.8688903 |
| 3 | 0.0833333 | 0.8688903 | 0.3500212 |

These were derived by Carlson by solving a nonlinear system of equations

$$\sum_{m=1}^{M} w_m\, \mu_m^{\ell}\, \eta_m^{p} = \int d\Omega \mu^{\ell} \eta^{p}, \qquad \ell,\ p \text{ even, and } \ell+p = 0,2,4 \qquad \text{(A-9)}$$

with the constraint of equal weights. Since Eq. (A-9) has a unique solution, the $\left[a^0_{m0}\right]$ of Eq. (A-8) and the $\left[w_m\right]$ of Eq. (A-9) must be identical except for a normalizing constant.

2. Quadrature Set 2--The second set, named the $ZP_N$ (zeroes of Legendre polynomial) set is found by solving the six nonlinear equations of Eq. (A-9) along with the three constraints that each $\mu_m$ be a zero of $Y^0_4$. The resulting set is

| m | $w_m$ | $\mu_m$ | $\eta_m$ |
|---|---|---|---|
| 1 | 0.0815181 | 0.3399810 | 0.3499611 |
| 2 | 0.0869637 | 0.8611363 | 0.3594757 |
| 3 | 0.0815181 | 0.3399810 | 0.8728896 |

Again, the equations to find the $ZP_N$ set have unique solutions. Thus, the weights and $\left[a^0_{m0}\right]$ must be equal to the $\left[w_m\right]$ except for normalization.